Available online at www.sciencedirect.com
SCIENCE DIRECT
Polymer 47 (2006) 2163–2171
polymer
www.elsevier.com/locate/polymer

Blends of styrene butadiene styrene TRI block copolymer/ polyaniline-Characterization by WAXS

F.G. Souza Jr [a], B.G. Soares [a,*], G.L. Mantovani [b], A. Manjunath [c], H. Somashekarappa [c], R. Somashekar [c], Siddaramaiah [d]

[a] *Instituto de Macromoleculas, Centro de Tecnologia, Universidade Federal do Rio de Janeiro, Bl. J, Ilha do Fundão, 21945-970, Rio de Janeiro, RJ, Brazil*
[b] *Instituto de Física, Universidade de São Paulo, São Carlos, SP, Brazil*
[c] *Department of Studies in Physics, University of Mysore, Manasagangotri, Mysore 570 006, India*
[d] *Department of Polymer Science and Technology, S.J. College of Engineering, Mysore 570 006, India*

Received 17 October 2005; received in revised form 12 January 2006; accepted 13 January 2006
Available online 7 February 2006

Abstract

Electrically conductive blends based on polyaniline-dodecylbenzene sulphonic acid (Pani.DBSA)/styrene–butadiene–styrene (SBS) block copolymer have been prepared by two methods namely melt mixing and polymerization of aniline in the presence of SBS using in situ polymerization method. The influence of composition and synthetic methods on the performance of SBS/Pani blends was established. The obtained SBS/Pani blends have been characterized by mechanical, morphological and electrical properties. A great reduction in volume resistivity values with increase in Pani content was noticed for in situ polymerization method compared to melt mixing method. The microstructural parameters were also computed using Wide Angle X-ray Scattering (WAXS). The results are compared with mechanical and electrical properties.

Keywords: Conducting composite; Polyaniline; WAXS

1. Introduction

Styrene–butadiene–styrene (SBS) block copolymer is well known thermoplastic–elastomer material, which presents the unique combination of the rubber properties and thermoplastic processability [1]. These characteristics make this copolymer an interesting host matrix for the development of conducting polymer systems through the dispersion of conducting fillers. Indeed, there are several studies in literature concerning blends of SBS with conducting carbon black [2] and conducting polymers as polypyrrol [3] and polyaniline [4–12].

Several methods have been employed to prepare SBS/polyaniline (Pani) blends and include solution mixing [11], mechanical mixing [4,8,10,12] and in situ polymerization of aniline in the presence of SBS solution [5–7,9]. The one step in situ polymerization is very attractive in comparison to the other conventional methods, because the last one involves several laboratory steps, that is, the polymerization of aniline in presence of functionalized protonic acid, followed by washing, drying and blending the polyaniline with the host polymer. In addition, the one step polymerization procedure provides an insulator–conductor transition at relatively low percolation threshold, for several other systems [6,13,14]. Some studies employ *p*-toluene sulfonic acid as the protonic acid in combination with a surfactant to stabilize the emulsion [5]. However, other papers perform the in situ polymerization of aniline in the presence of the host insulating polymer, using dodecylbenzene sulfonic acid (DBSA), which acts simultaneously as emulsifier and dopant [6,7,9]. In this case, it is not necessary to add an external surfactant to achieve stable emulsion.

The method use to prepare SBS/Pani.DBSA blends exerts strong influence on the electrical properties. For example, mechanical mixing of SBS with Pani.DBSA (prepared by redoping process) resulted in a light insulator–conductor transition [10], whereas solution blends [11] or that obtained by in situ polymerization [6] provide sharp transition. The different electrical behavior may be related to the extent of ordered solid state structure such as crystalline domains that polyaniline chains assume inside the SBS matrix, when the blends are prepared by different procedures.

* Corresponding author. Tel./fax: +55 2125627207.
E-mail address: bluma@ima.ufrj.br (B.G. Soares).

0032-3861/$ - see front matter © 2006 Elsevier Ltd. All rights reserved.
doi:10.1016/j.polymer.2006.01.033

Wide angle X-ray scattering (WAXS) studies constitute important tool for the determination of crystallinity extent of polyaniline and also other important microcrystalline parameters which help to understand some peculiar electrical behavior of polyaniline and their blends [15–19].

The present paper investigates the influence of blending procedure on the electrical, morphological and mechanical properties of SBS/Pani.DBSA blends. The effect of SBS on the crystallinity and microstructural parameters of Pani.DBSA was also evaluated by WAXS. For blends prepared by mechanical mixing, it was employed Pani.DBSA synthesized by one step emulsion polymerization in toluene. These reaction conditions were similar to that used for the preparation of in situ polymerized aniline-based blends and were chosen in order to keep the same Pani characteristics in both blend systems.

2. Experimental

2.1. Materials

SBS (TR-1061; PBD content = 70 wt%; $\langle M_w \rangle$ = 120,000 g/mol; density = 0.98 g/cm^3) was kindly supplied by Petroflex S.A. (Rio de Janeiro, Brasil). Aniline (Ani) (analytical grade from Vetec, Brazil), ammonium peroxydisulfate (APS) (analytical grade from Vetec, Brazil) and dodecylbenzene sulfonic acid (DBSA) (commercial grade from Solquim LTDA, Brazil) were used without further purification.

2.2. Synthesis of polyaniline doped with DBSA (Pani.DBSA)

Pani.DBSA used in mechanical mixing was synthesized by one-step route in toluene according to the procedure reported elsewhere [20,21]. In a typical procedure, 4.7 mL (0.051 mol) of aniline and 16.7 g (0.051 mol) of DBSA were dissolved into 250 mL of toluene under constant stirring. The reaction mixture was kept at 0 °C and an aqueous solution containing 11.36 g (0.051 mol) of APS in 40 mL of water was slowly added over a period of 20 min. After 6 h, the reaction medium was poured into a nonsolvent like methanol, filtered, washed several times with methanol and dried.

2.3. Blend preparation

2.3.1. Melt mixing method

Different amount of SBS copolymer was first introduced into a Haake Rheocord 9000 internal mixer operating with a Cam rotor at 100 °C and 60 rpm. After 2 min, Pani.DBSA powder was added and mixing was continued for 8 min. The blends were then quickly sheeted in a two-roll mill.

2.3.2. In situ polymerization method

A 10% solution of SBS in toluene was first prepared. Then, different amount of aniline (Ani) and DBSA were added under stirring. The reaction medium was kept at 0 °C and an aqueous solution of APS was added dropwise into the emulsion, with stirring. The APS/Ani/DBSA molar ratio was 1:1:1.

2.4. Mechanical testing and characterization

The samples for tensile tests were compression molded into sheets (80 × 80 × 2 mm) at 100 °C, for 3 min under the pressure of 4.5 ton. Tensile experiments were performed in an Instron 5569 tensile machine (Boston, MA) at room temperature in accordance to ASTM D638. The conditions used were pneumatic claw with separation velocity of 100 mm/min; 7.62 mm between the marks; at room temperature of 24 °C.

The samples for volume resistivity were prepared by compression-molding the composites in disk molds with 38 mm diameter, at 100 °C, for 3 min, using a force of 4.5 ton. The ASTM D257 procedure was used for determination of the volume resistivity, Rv. All measurements were performed with a Keithley 6517A electrometer.

The morphology of the samples was determined by scanning electron microscopy (SEM) on a JEOL equipment model JSM-5300 with 10 kV of voltage acceleration. The micrographs were taken from cryofracturated surfaces after coating with a thin layer of gold.

The ultraviolet–visible spectrometry measurements were performed on a Varian UV–vis Spectrometer Model CARY 100. The samples were dissolved in toluene in a concentration of 5.5×10^{-5} g/ml.

The X-ray scattering measurements were performed at the WAXS/SAXS beam line of the LNLS (Laboratório Nacional de Luz Sincroton—Campinas, Brazil), by using monochromatic beam of wavelength 1.7433 Å. The scattering intensity was registered using a one dimensional position-sensitive gas detector for a sample-detector distance of 1641.5 mm. In case of WAXS, 2θ degree corrections were done against Al_2O_3 pattern. The scan range (2θ) was 2–80°. WAXS curves were obtained from the WAXS images by band integration tool supplied by X-ray 1.0 software, produced by Université Mons Hainaut.

3. X-ray background to determine the microcrystalline parameters

Microstructure encompasses the compositional inhomogeneity, the amount and distribution of the phase in the material, the grain size and shape and the distribution functions of the grain-size parameters, the grain (crystal)-orientation distribution function (texture), the grain boundaries/interfaces and the surface of the material.

Microstructural parameters like crystal size $\langle N \rangle$ and lattice strain (lattice disorder) (g in %) are usually determined by employing Fourier method of Warren and Averbach [22] and Warren [23,24]. The intensity of a profile in the direction from the origin to the center of the reflection can be expanded in terms of Fourier cosine series as:

$$I(s) = \sum_{n=-\infty}^{\infty} A(n)\cos\{2\pi nd(s - s_0)\} \quad (1)$$

where the coefficients of the harmonics $A(n)$ are functions of the size of the crystallite and the disorder of the lattice. Here, s

is (sin θ)/λ, s_0 is the value of s at peak of a profile, n is coefficient of the harmonic order and d is the lattice spacing. The Fourier coefficients can be expressed as:

$$A(n) = A_s(n) \times A_d(n) \tag{2}$$

For a paracrystalline material, $A_d(n)$ turns out to Warren [24] and Hall [25] statement, with Gaussian strain distribution,

$$A_d(n) = \exp(-2\pi^2 m^2 n g^2) \tag{3}$$

where m is the order of the reflection and $g=(\Delta d/d)$ is the lattice strain. Normally one also defines mean square strain $\langle \varepsilon^2 \rangle$ that is given by g^2/n. This mean square strain is dependent on n, whereas not g [26,27]. For a probability distribution of column lengths $P(i)$, we have

$$A_s(n) = 1 - \frac{nd}{D} - \frac{d}{D}\left[\int_0^n iP(n)\mathrm{d}i - n\int_0^n P(i)\mathrm{d}i\right] \tag{4}$$

where $D=\langle N \rangle d_{hkl}$ is the crystallite size and i is the number of unit cells in a column.

In the presence of two orders of reflections from the same set of Bragg planes, Warren and Averbach [22] have shown a method of obtaining the crystal size ($\langle N \rangle$) and lattice strain (g in %). But in polyaniline material it is not common to find multiple reflections. So, to find the finer details of microstructure, we approximate the size profiles by simple analytical function for $P(i)$. Here we have considered only asymmetric functions. Another advantage of this method is that the distribution function is different along different directions. According to Ribarik et al., Pope et al. and Scardi et al. [28–30], a single crystal size distribution function is used for the whole pattern fitting which we feel, may be inadequate to describe polyaniline diffraction patterns. It is important to emphasize that the Fourier method of profile analysis (Single order method) used in this paper was proved to be quite reliable in a recent survey and results of Round Robin test conducted by IUCr [29]. In fact, for refinement, we have also considered the effect of background by introducing a parameter (see for details regarding the effect of background on the microcrystalline parameters) [30].

3.1. The exponential distribution

It is assumed that there are no columns containing fewer than p unit cells and those with more decay exponentially. Thus, we have [31]:

$$P(i) = 0; \qquad p < i \tag{5}$$

$$P(i) = \alpha \exp\{-\alpha(i-p)\}; \quad i \geq p \tag{6}$$

where, $\alpha = 1/(N-p)$.

Substituting this in Eq. (4), we get:

$$A_s(n) = A(0)(1 - n/\langle N \rangle); \qquad n \leq p \tag{7}$$

$$A_s(n) = A(0)\{\exp[-\alpha(n-p)]\}/\alpha\langle N \rangle; \quad n \geq p \tag{8}$$

Here α is the width of the distribution function, i is the number of unit cells in a column, n is the harmonic number, $\langle p \rangle$ is the smallest number of unit cells in a column and $\langle N \rangle$, the number of unit cells counted in a direction perpendicular to the (hkl) Bragg plane. The exponential distribution function was introduced in order to find out the most suitable crystal size distribution function for the profile analysis of the X-ray fiber diffraction. The procedure adopted for the computation of the parameters is as follows: Initial values of g and N were obtained using the method of Nandi et al. [27]. With these values obtained from the equations mentioned earlier in the text, the corresponding values for the width of distribution are calculated. These are only rough estimates, so the refinement procedure must be sufficiently robust to start with such values. Here, we compute

$$\Delta^2 = \frac{[I_{cal} - (I_{exp} + BG)]^2}{npt} \tag{9}$$

where BG parameter represents the error in the background estimation, npt is number of data points in a profile, I_{cal} is intensity calculated using Eq. (1) and I_{exp} is the experimental intensity. The values of Δ were divided by half of the maximum value of intensity. Therefore, it is expressed relative to the mean value of intensities, and then minimized. For refinement against intensities, the multi-dimensional minimization algorithm of the SIMPLEX method was used [32].

4. Results and discussion

4.1. Electrical and mechanical properties

Table 1 presents the effect of feeding ratio of Ani-SBS on the Pani.DBSA content in blends and yield, both which were calculated gravimetrically. For relatively low amount of aniline, the Pani yield increased with the increase of feeding weight ratio of Ani-SBS. However, for high weight ratio of Ani-SBS (0.41) there is a decrease of yield. Table 2 compares the tensile properties and electrical resistivity of SBS/Pani.DBSA blends obtained by different procedures. The presence of Pani.DBSA drastically reduced the ultimate properties (tensile strength and elongation at break), whatever be the method used for the blend preparation. This behavior may be attributed to the interactions between the Pani molecules with the SBS matrix, which contribute for the reduction of physical crosslink strength of polystyrene domains of SBS block copolymer. Therefore, the thermoplastic–elastomer characteristics of SBS are lost, affecting the mechanical properties. Blends prepared by in situ polymerization displayed lower values of elongation at break and significant higher surface hardness, indicating a higher extent

Table 1
Effect of the feeding ratio of Ani-SBS on the yield of Pani.DBSA and blend composition

Feeding ratio of Ani-SBS (wt/wt)	Pani.DBSA content in the composite (wt%)	Yield of Pani.DBSA (%)
10/100	16.2	67
21/100	32.3	84
41/100	43.9	70
60/00	–	66

Table 2
Tensile properties, hardeness and electrical resistivity of SBS/Pani.DBSA blends obtained by different procedures

Blend composition		Ultimate tensile strength (MPa)		Elongation at break (%)		Surface hardness (shore-A)		Volume resistivity (ohm cm)	
SBS (%)	Pani.DBSA (%)	Physical blend	In situ polym	Physical blend	In situ polym	Physical blend	In situ polym	Physical blend	In situ polym
100	0	16.8±1.1	16.8±1.1	1022±17	1022±17	73±2	73±2	$(2.85\pm0.8)\times10^{12}$	$(2.85\pm0.8)\times10^{12}$
85	15	7.2±0.3	4.6±0.9	597±68	216±54	67±2	75±3	$(6.33\pm0.3)\times10^{12}$	$(3.10\pm0.03)\times10^{5}$
70	30	2.4±0.8	3.7±0.4	192±62	179±60	65±2	78±4	$(2.92\pm0.07)\times10^{6}$	$(3.57\pm0.01)\times10^{4}$
55	45	2.0±0.2	3.0±0.1	128±21	75±35	59±3	84±1	$(8.33\pm0.04)\times10^{4}$	$(1.40\pm0.01)\times10^{4}$
0	100	–	–	–	–	–	–	$(9.0\pm0.8)\times10^{0}$	$(9.0\pm0.8)\times10^{0}$

of interaction between the components and the formation of a physical interpenetrating network involving Pani and SBS chains. The effective entanglement between Pani chains contributes for the embrittlement of the material, because of the brittle nature of polyaniline.

Blends prepared by in situ polymerization also displayed lower values of resistivity. With 15% of Pani.DBSA, the difference in resistivity was around 10^7 of magnitude, indicating an insulator–conductor transition at lower percolation threshold. The better electrical performance of in situ polymerized aniline-based blends may be related to favorable morphology.

4.2. Morphology

Fig. 1 compares the SEM micrographs of SBS/Pani.DBSA (85:15 wt%) blends prepared by both methods. In blend prepared by mechanical mixing, Pani.DBSA is heterogeneously distributed in the form of agglomerates (Fig. 1(a)). On the other hand, that prepared by in situ polymerization presented a more homogeneous distribution of Pani.DBSA component, with the formation of very thin microtubules (most of them with less than 1 μm diameter) interconnected each other thus forming the conducting pathway, which is responsible for the improved conductivity. This is better observed in the micrograph taken at higher magnification (Fig. 1(b)).

4.3. UV-vis spectroscopy

Besides the morphological characteristics, the higher resistivity values found in blends prepared by mechanical mixing should be also due to a dedoping process, which may take place during processing the blends in the Haake internal mixer. UV-vis spectroscopy is an important tool for the evaluation of the doping level of polyaniline [33,34]. Fig. 2 compares the UV-vis absorption spectra of SBS/Pani.DBSA blends prepared by different procedures. In both systems, three characteristic absorption peaks are observed: at around 350 nm, which is ascribed to π–π* transition of the benzenoid rings, and at 400–420 and 750–800 nm, attributed to

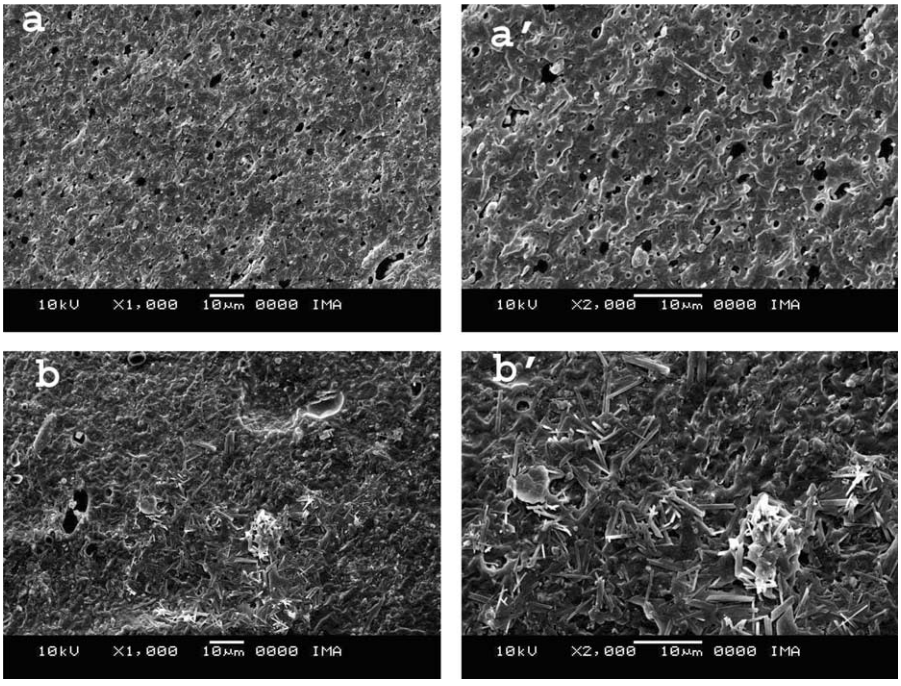

Fig. 1. SEM micrographs of SBS/Pani.DBSA (85:15 wt%) blends prepared by (a) mechanical mixing and, (b) in situ polymerization of aniline.

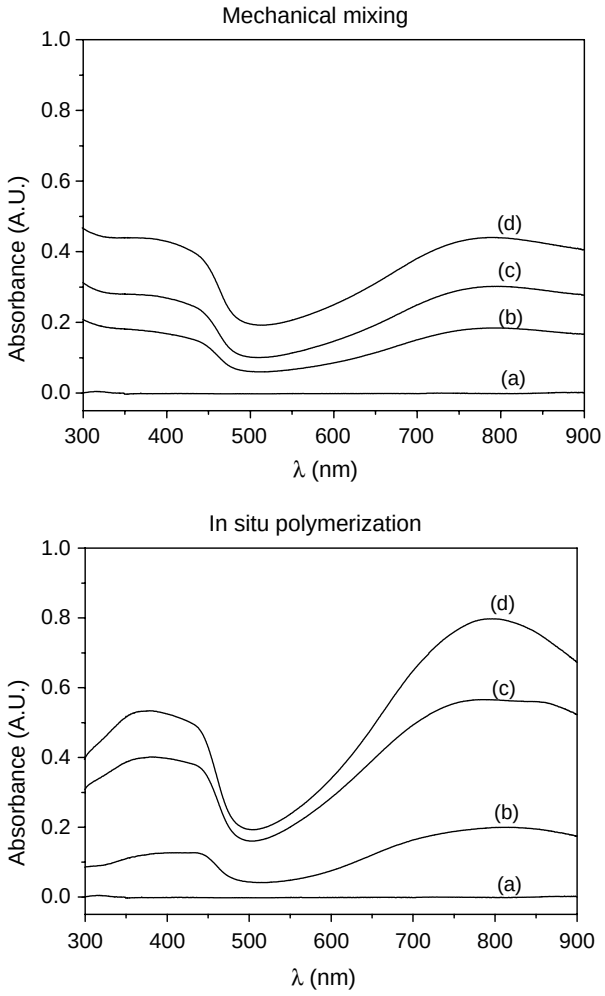

Fig. 2. UV-vis absorption spectra of (a) SBS and their blends with, (b) 15%, (c) 30% and, (d) 45% of Pani.DBSA, prepared by mechanical mixing and in situ polymerization of aniline.

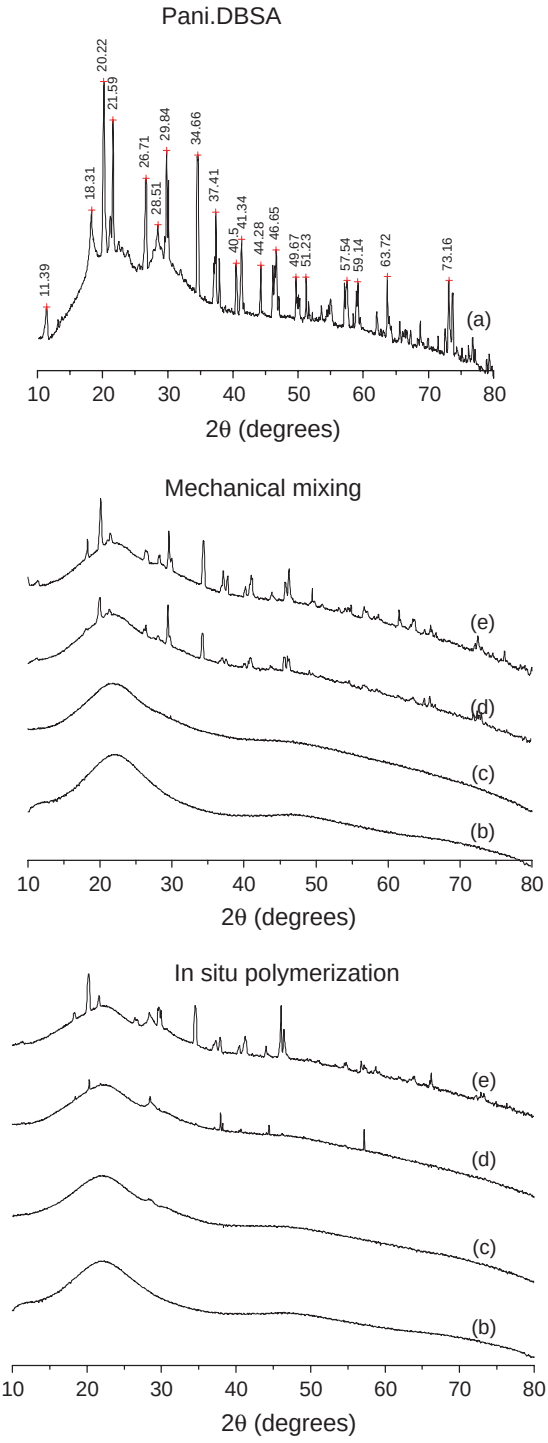

Fig. 3. WAXS patterns of (a) Pani.DBSA, (b) SBS and their blends containing, (c) 15%, (d) 30% and, (e) 45% of Pani.DBSA, prepared by mechanical mixing and in situ polymerization.

polaron-π* transition and π-polaron transition, respectively [34–36]. The peak at higher wavelength is related to the doping level and formation of polaron [37]. The extent of doping can roughly be estimated from the ratios of the absorbance intensity at 750–800 nm (π-polaron) and around 350 nm (π–π* transition) [33,34]. Blends prepared by in situ polymerization presented a ratio around 1.4. This value is close to that found for pure Pani.DBSA prepared by emulsion process and did not change with the blend composition. Blends prepared by mechanical mixing displayed smaller intensity ratio (around 0.9) in all blend composition studied, which suggests lower doping level. Since these intensity ratios are smaller than that of pure Pani.DBSA used to prepare these blends, one can suggest that the decreasing on the doping level in mechanical mixer blends occurs during processing in the Haake.

4.4. X-ray profile analysis

X-ray diffractograms recorded for Pani, SBS and both series of their blends, are shown in Fig. 3. Pani.DBSA diffractrogram presented several sharp reflections. The most important of them include those at $2\theta = 20.21$, 21.59, 26.66, 29.84 and 34.60°. On the other hand, the diffractogram of the amorphous SBS sample displayed only one broad maximum at $2\theta = 22.18°$. The blends also displayed multiple sharp reflections whose number and size depend upon the

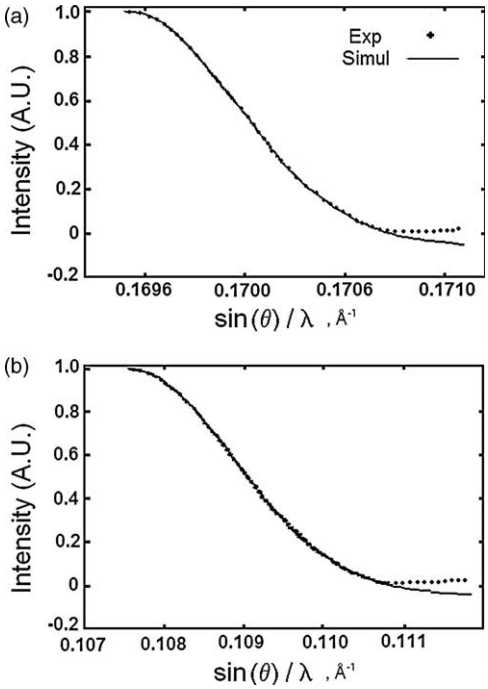

Fig. 4. Experimental and simulated X-ray profiles for SBS/Pani.DBSA (55:45 wt%) blends obtained by (a) mechanical mixing and, (b) in situ polymerization.

composition of Pani.DBSA in the blends and also the method used for blend preparation. Blends containing 15% of Pani.DBSA presented a diffractogram similar to that found in pure SBS, indicating very low crystallinity level. As the Pani.DBSA content in the blend increases, sharp peaks started to appear, as a consequence of an increase on crystalline dispersed phase of Pani in amorphous SBS matrix. For the same Pani.DBSA content, the blend prepared by in situ polymerization displayed less number of peaks, indicating lower crystallinity level and different molecular arrangements/crystal structures. The higher crystallinity level in blends prepared by mechanical mixing may be attributed to the self-assembly of Pani molecules into aggregates. This phenomenon occurs in less extension in the case of blends prepared by in situ polymerization due to the higher degree of dispersion of Pani.DBSA.

The broadening of X-ray reflections observed in these SBS/Pani.DBSA blends is attributed to microdefects [38], which also contribute for the decreasing in crystal size ($\langle N \rangle$) and increase in lattice strain or lattice disorder (g in %). The number of unit cells (crystal size, $\langle N \rangle$) counted in a direction perpendicular to the Bragg's plane is 128.15 for Pani and around 3.40 units for SBS. The $\langle N \rangle$ values of blends lie between Pani and SBS values. Along with this, there is also a lattice disorder of second kind, known as paracrystallinity, and

Table 3
Microstructural parameters of SBS, Pani and their blends obtained from WAXS data employing exponential distribution function

Blend composition (SBS/Pani), (wt/wt, %)	2θ (degrees)	D (Å)	$\langle N \rangle$[a]	g (%)[b]	α[c]	D_s (Å)[d]	δ	α*[e]
0/100	20.21	2.523						
	21.59	2.369						
	26.66	1.943	128.15	0.4	4.5281	443.12	0.05	4.53
	29.84	1.752						
	34.60	1.535						
100/0	22.18	2.309	3.40	0.5	0.9220	15.4	0.05	0.92
(a) Blends preparation by melt mixing								
85/15	21.85	2.342	3.48	0.5	0.9327	16.0	0.05	0.93
70/30	20.10	2.536						
	21.07	2.425	107.4	0.5	5.1817	379.5	0.06	5.18
	29.39	1.776						
	34.24	1.549						
55/45	18.25	2.783						
	29.56	1.767						
	20.09	2.538	107.6	0.3	3.1119	438.26	0.04	3.10
	34.35	1.545						
(b) Blends preparation by in situ polymerization method								
83.8/16.2	21.95	2.332	3.92	0.5	0.9899	17.94	0.03	0.99
67.7/32.3	20.43	2.497						
	21.57	2.371	13.37	0.3	1.0970	60.34	0.05	1.09
	28.29	1.839						
56.1/43.9	18.33	2.772						
	20.21	2.523	41.8	0.2	1.2931	60.34	0.04	1.29
	21.61	2.367						

[a] Number of unit dells (crystal size).
[b] Lattice strain.
[c] Width of the crystal size distribution.
[d] Surface weighted crystal size.
[e] Enthalpy.

normally quantified as strain ($g = \Delta d/d$), where 'd' is the inter planar spacing. The microcrystalline parameters were estimated by simulating the experimental profile, employing the procedure described earlier [39,40]. Fig. 4 illustrates the simulated and experimental profile for SBS/Pani.DBSA (55:45 wt%) blends obtained by different procedures. It is evident from this figure that the experimental data and the model parameters based on exponential distribution function are quite reliable. This method of obtaining microstructure parameters was also reliable in other systems [31,41].

The microcrystalline parameters obtained by Fourier and simulation method are listed in Table 3, for SBS/Pani.DBSA blends with different compositions. The order of magnitude of the surface-weighted crystal size (D_s) indicates the extent of crystallinity present in surface. From Table 3, it is evident that the microcrystalline parameters, such as D_s and number of unit cells ($\langle N \rangle$), increase with the increase of Pani content in the blends. From $\langle N \rangle$ and g parameters, the enthalpy (α^*) was calculated, using Hosemann's paracrystalline disorder model [40]:

$$\alpha^* = \langle N \rangle^{1/2} g \tag{10}$$

The results also presented in Table 3 indicate an increase of the enthalpy with increase in percent of Pani content in the blend matrix. This behavior was significant in blends with 30% of Pani and prepared by physical mixing. This behavior is also an indication of the increase of the crystalline region. This implies that a more ordered polymer network needs more strength (external) or energy to disturb the system.

It is important to point out that blends prepared by in situ polymerization, which presented lower values of resistivity, also displayed smaller crystal size, lower lattice strain values and lower enthalpy. In addition, it was observed a substantial decrease on surface-weighted crystal size (D_s). All these results indicate a decrease on crystallinity level. Blends prepared by this method can be considered a physical interpenetrating network. Therefore, large aggregates constituted by Pani chains do not form in large extent because of the interconnection of SBS chains. The absence of large aggregates decreases the crystallinity level but promotes the formation of conducting pathway at lower Pani concentration (lower percolation threshold). The in situ polymerization improves the distribution of Pani chains inside the SBS matrix, thus increasing the disorder of the polymer network [41,42]. The conductivity associated with the free ion increases because of a lower potential barrier.

Fig. 5 shows the ellipsoid shape of crystallite inside the samples. From these figures it was noticed that, the D_s curve shape decreases with increase in Pani content for the blends prepared by both synthetic methods. The variation of $\langle N \rangle$ and tensile strength with composition of Pani is shown in Fig. 6(a) and (b) for melt mixing and chemical method respectively. The plot of $\langle N \rangle$ and volume resistivity as a function of Pani content is shown in Fig. 7(a) and (b) for melt and chemical methods respectively. From these figures, it is evident that the increase

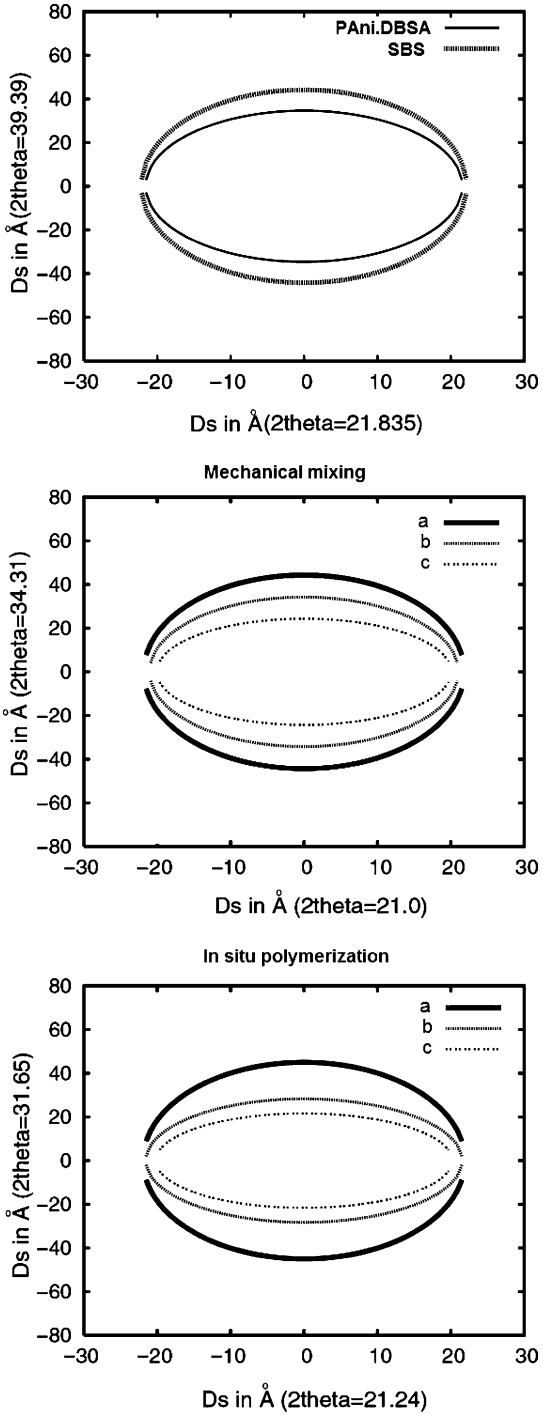

Fig. 5. The crystallite ellipsoid shape of the SBS, Pani.DBSA and SBS/Pani.DBSA blends with (a) 15%; (b) 30% and, (c) 45% of Pani.DBSA.

in crystallite size causes a decrease in tensile strength and volume resistivity, associated with slight reduction in lattice disorder measured in terms of the 'g' parameter. With incorporation of Pani into SBS, we find that from X-ray recordings and also from our results that there is an increase in crystalline order with increase in Pani, which results in increase of London force in a direction perpendicular to the drawing of the films.

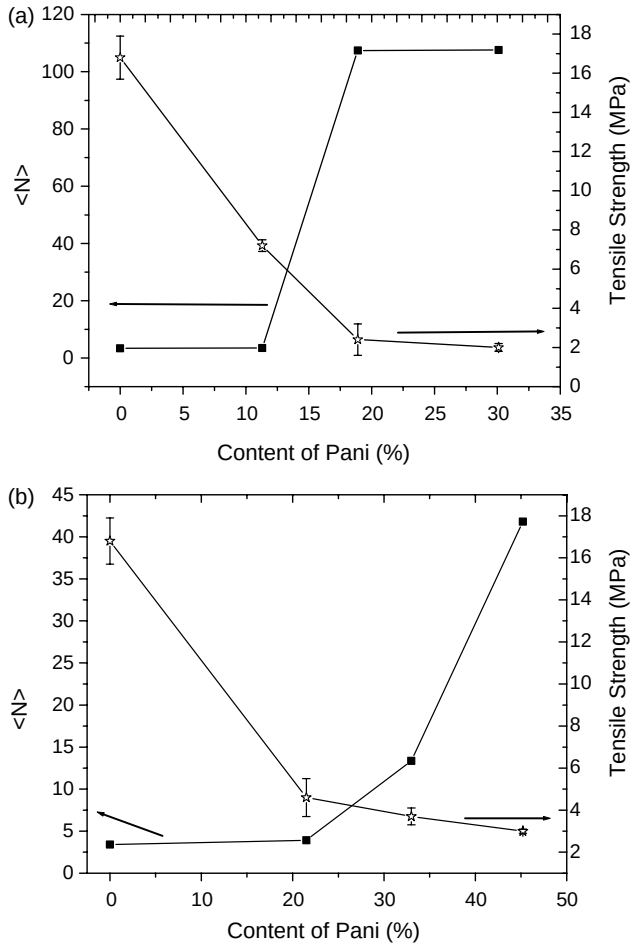

Fig. 6. Variation of crystal ⟨*N*⟩ and tensile strength as a function of the Pani content; (a) Melt mixing and, (b) in situ polymerization method.

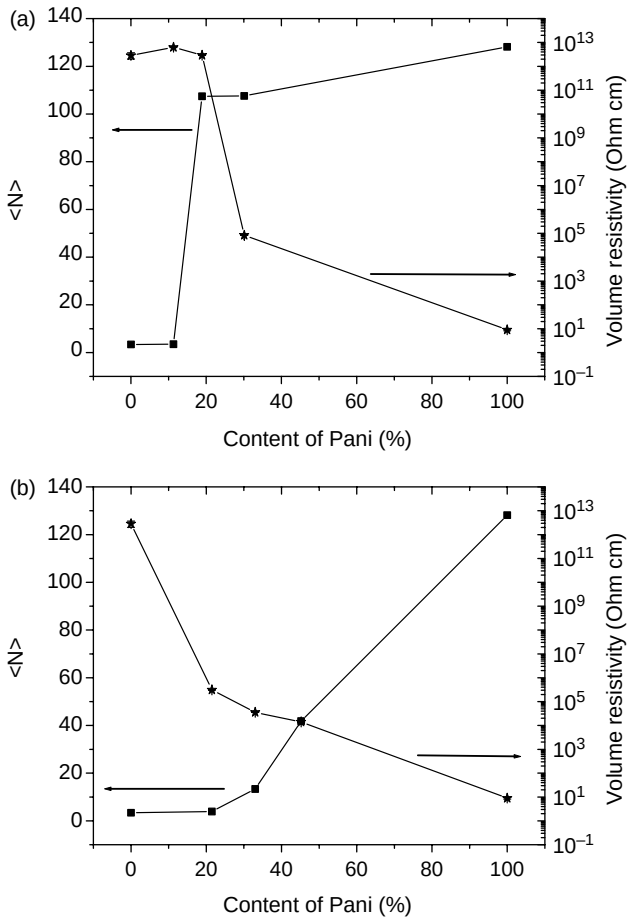

Fig. 7. Plots of ⟨*N*⟩ and volume resistivity as a function of the Pani content. (a) Melt mixing and, (b) in situ polymerization method.

5. Conclusions

In the present work, the influence of synthetic routes on the microcrystalline behavior of SBS/Pani blends has been studied by WAXS. The ⟨*N*⟩ value increases with increase in crystalline Pani content in the amorphous SBS matrix, as expected. The tensile strength and volume resistivity decrease with increase in Pani content, whereas ⟨*N*⟩ value increases. This is due to increase in high crystalline Pani phase in SBS matrix. The changes in physical properties are attributed to the crystal imperfection, wherein parameters like ⟨*N*⟩ and D_s increase with increase in Pani content.

Blend prepared by in situ polymerization resulted in lower resistivity because of a favorable morphology characterized by the formation of interconnected microtubules, which form the conducting pathway with lower amount of Pani. In spite of lower resistivity, the crystallinity level of these blends was lower than the corresponding mechanical mixing blends. Blends prepared by in situ polymerization method can be considered a physical interpenetrating network. Therefore, there was no formation of large aggregates constituted by Pani chains in large extent because of the interconnection of SBS chains. The absence of large aggregates decreases the crystallinity level but promotes the formation of conducting pathway at lower Pani concentration (lower percolation threshold).

Acknowledgements

We would like to acknowledge the Conselho Nacional de Desenvolvimento Científico e Tecnológico (CNPq), Coordenação de Aperfeiçoamento de Pessoal de Ensino Superior (CAPES) and Fundação de Amparo a Pesquisa do Estado do Rio de Janeiro (FAPERJ-26/150.351/2004), for the financial support for this project, and Third World Academy of Science (TWAS)-UNESCO for the fellowship to Prof. Siddaramaiah to visit Brazil. The author would like to thank Laboratório Nacional de Luz Sincontron for the technical support on the WAXS experiments (Research proposals D11A-SAS 2934/04 and D11A-SAXS No.3406/05).

References

[1] Holden G, Legge NR.,Holden G, Legge NR, Quirk R, Schroeder HE, editors. Styrenin thermoplastic elastomers. Thermoplastic elastomers, 2nd ed, vol. 47. New York: Hanser; 1996 (chapter 3).
[2] Leyva ME, Barra GMO, Moreira ACF, Soares BG, Khastgir D. J Polym Sci: Part B: Polym Phys 2003;41:2983.
[3] Ruckenstein E, Hong LA. Synth Met 1994;66:249.

[4] Davies SJ, Ryan TG, Wilde CJ, Beyer G. Synth Met 1995;69:209.
[5] Ruckenstein E, Sun Y. Synth Met 1995;74:107.
[6] Xie HQ, Ma YM, Guo JS. Polymer 1998;40:261.
[7] Xie HQ, Ma YM. J Appl Polym Sci 2000;77:2156.
[8] Cruz-Estrada RH, Folkes MJ. J Mater Sci 2000;35:5065.
[9] Xie HQ, Ma YM, Guo JS. Synth Met 2001;123:47.
[10] Leyva ME, Barra GMO, Gorelova MM, Soares BG. J Appl Polym Sci 2001;80:626.
[11] Leyva ME, Barra GMO, Soares BG. Synth Met 2001;123:443.
[12] Leyva ME, Soares BG, Khastgir D. Polymer 2002;43:7505.
[13] Xie HQ, Ma YM. J Appl Polym Sci 2000;76:845.
[14] Xie HQ, Pu QL, Xie D. J Appl Polym Sci 2004;93:2211.
[15] Pouget JP, Józefowicz ME, Epstein AJ, Tang X, MacDiarmid AG. Macromolecules 1991;24:779.
[16] Chaudhari HK, Kelkar DS. J Appl Polym Sci 1996;62:15.
[17] Pouget JP, Hsu CH, MacDiarmid AG, Epstein AJ. Synth Met 1995;69: 119.
[18] Luzny W, Banka E. Macromolecules 2000;33:425.
[19] Minto CDG, Vaughan AS. Polymer 1997;38:2683.
[20] Osterholm JE, Cao Y, Klavetter F, Smith P. Polymer 1994;35:2902.
[21] Barra GMO, Leyva ME, Gorelova MM, Soares BG, Sens M. J Appl Polym Sci 2001;80:556.
[22] Warren BE, Averbach BL. J Appl Phys 1950;21:595.
[23] Warren BE. Acta Cryst 1955;8:483.
[24] Warren BE. X-ray diffraction. New York: Addision-Wesley; 1969.
[25] Hall IH, Somashekar R. J Appl Crystallogr 1991;24:1051.
[26] Rothman RL, Cohen JB. J Appl Phys 1971;24:971–9.
[27] Nandi RK, Kho HK, Schlosberg W, Wissler G, Cohen JB, Crist Jr B. J Appl Crystallogr 1984;17:22.
[28] Ribarik R, Ungar T, Gubicza J. J Appl Crystallogr 2001;34:669.
[29] Pope NC, Balzar D. J Appl Crystallogr 2002;35:338.
[30] Scardi P, Leoni M. Acta Crystallogr A 2001;57:604.
[31] Somashekar R, Hall IH, Carr PD. J Appl Crystallogr 1989;22:363.
[32] Numerical Recipes. In: Press W, Flannery BP, Teukolsky S, Vetterling WT, editors. Cambridge: Cambridge University Press; 1986.
[33] Abdiryim ZX, Gang ZX, Jamal R. Mater Chem Phys 2005;90:367.
[34] Xia HS, Wang Q. J Nanopart Res 2001;3:401.
[35] Epstein AJ, Ginder JM, Zuo F, Bigelow RW, Woo HS, Tanner DB, et al. Synth Met 1987;18:303.
[36] Wei Y, Hsuech FK, Jang GW. Macromolecules 1994;27:518.
[37] MacDiarmid AG, Epstein AJ. Synth Met 1994;65:103.
[38] Mallu P, Siddaramaiah, Somashekar R. Bull Mater Sci 2000;23:413.
[39] Murthy NS, Wang ZG, Hsiao BS. Macromolecules 1999;32:5594.
[40] Hosemann R. Prog Colloid Polym Sci 1988;77:15.
[41] Jeevananda T, Siddaramaiah, Annadurai V, Somashekar R. J Appl Polym Sci 2001;82:383.
[42] Jeevanda T, Siddaramaiah, Somashekarappa H, Somashekar R. J Appl Polym Sci 2002;83:1730.